Electronic structure of $ThBe_{13}$

N. Harrison
National High Magnetic Field Laboratory, LANL, MS-E536, Los Alamos, New Mexico 87545

A. L. Cornelius
MST-10, Los Alamos National Laboratory, Los Alamos, New Mexico 87545

H. Harima
The Institute of Scientific and Industrial Research, Osaka University, Ibaraki, Osaka 567-0047, Japan

K. Takegahara
Department of Materials Science and Technology, Hirosaki University, Hirosaki, Aomori 036-8561, Japan

J. A. Detwiler and G. M. Schmiedeshoff
Department of Physics, Occidental College, Los Angeles, California 90041

J. C. Cooley and J. L. Smith
Superconductivity Technology Center, Los Alamos National Laboratory, Los Alamos, New Mexico 87545
(Received 17 August 1999)

Angle-resolved de Haas–van Alphen measurements made on $ThBe_{13}$ in pulsed magnetic fields are compared with Fermi surface predictions calculated by means of the linear augmented-plane-wave method with spin-orbit interactions. While all of the experimentally determined quasiparticle effective masses are light and of order the free electron mass, they are still roughly double those obtained from the calculated band structure, thereby being suggestive of the existence of notable electron-phonon interactions. The relevance of these de Haas–van Alphen results to strongly correlated UBe_{13} is also discussed.

I. INTRODUCTION

Rare earth and actinide beryllides in the form MBe_{13} provide an interesting series of compounds for the study of strongly correlated electron effects in metals.[1] Crystallizing in the $O_h^6 Fm3c$ space group, they have large cubic unit cells comprised of 8 formula units, with lattice parameters exceeding 10 Å.[2] UBe_{13} is perhaps the most exotic compound within this series and the most often cited, having one of the highest electronic specific heats ($\gamma \sim 1100$ mJmol^{-1}K^{-2}) among heavy fermion compounds,[3–5] a novel superconducting ground state[1,3] ($T_c \sim 0.85$ K) and non-Fermi-liquid-like properties[6–8] (at least at low fields $B < 9$ T). $NpBe_{13}$, on the other hand, is an antiferromagnetically ordered heavy fermion system ($\gamma \sim 900$ mJmol^{-1}K^{-2}),[9,10] while $CeBe_{13}$ is a dense Kondo compound with only a moderately enhanced specific heat ($\gamma \sim 115$ mJmol^{-1}K^{-2}).[11] $LaBe_{13}$ and $ThBe_{13}$, by comparison, have much lower electronic specific heats ($\gamma \lesssim 10$ mJmol^{-1}K^{-2}),[1] more typical of ordinary metals.

In spite of the fact that compounds of this series have been studied for more than two decades, studies of Landau quantum oscillations (LQO's) are very much incomplete. Both magnetoacoustic[12] and de Haas–van Alphen[13] (dHvA) oscillatory effects have been reported in UBe_{13}. However, the characteristic effective masses were found to be anomalously low compared to other heavy fermion systems,[14] and the very existence of LQO's clearly contradicts the arguments that have been made for a non-Fermi-liquid ground state.[6–8] Following a comment, that was published in which it was suggested that the oscillations may have originated from Al flux inclusions[15] left over from the growth procedure, these dHvA results have since become controversial. Thus, we are left without definitive measurements of the dHvA effect in any MBe_{13} compound, yet the importance of such measurements for investigating Fermi-liquid properties cannot be over stressed. Studies of LQO effects in conjunction with band-structure calculations are necessary both for understanding the topology of the Fermi surface (FS),[16] should this exist, and the strong interactions that arise owing to the presence of partially delocalized f electrons.[17]

While $ThBe_{13}$ clearly does not exhibit the same strong correlations that occur in UBe_{13} or $NpBe_{13}$, it is of considerable interest because of the close proximity of Th to both U and Np in the periodic table. The lattice parameters in all of these beryllides are the same to within 1%,[1] so $ThBe_{13}$ may therefore be considered as the noninteracting analogue of the two aforementioned heavy fermion compounds. Band structure calculations in which the $5f$ electrons are considered to be itinerant,[2] predict the Fermi surface of UBe_{13} to be significantly different from that of $ThBe_{13}$. However, experimental investigations of the behavior of other heavy fermion compounds in a magnetic field have shown that their measured FS topologies often revert, at sufficiently strong fields (particularly above a metamagnetic transition), to one that is in closer correspondence with band-structure calculations in which the f electrons are localized.[18–20] From a theoretical perspective,[21,22] the modification of the FS and the accompanying saturation of the magnetization, on traversing a meta-

magnetic transition in heavy fermion compounds, is generally expected to result from Zeeman terms within the Hamiltonian. While a distinct metamagnetic transition has yet to be identified in pure UBe_{13},[23,24] measurements made in very strong magnetic fields have shown that the magnetization tends towards saturation at fields above ~ 60 T,[24] and given that the magnetic and quasiparticle properties of heavy fermion materials are inextricably linked, this signals a probable change in the electronic structure at high-magnetic fields.

Comparisons between UBe_{13} and $ThBe_{13}$ become particularly relevant when we consider changes to the ground-state properties of UBe_{13} induced by doping. Only when UBe_{13} is doped with Th, so as to make $U_{1-x}Th_xBe_{13}$,[25] is the suppression of T_c with x nonmonotonic. Two (or even three[26]) distinct phases of superconductivity are believed to exist for x in the range $0.02 \lesssim x \lesssim 0.04$,[27–29] accompanied by a further enhancement of the electronic contribution to the specific heat.[30] The FS together with the accompanying interactions are likely to vary in a continuous fashion with x.[20] A more complete understanding of the strong correlations in this series of intermetallics therefore necessitates a knowledge of the FS of noninteracting $ThBe_{13}$ as well as that of strongly interacting UBe_{13}.

In this paper we report measurements of the dHvA effect in $ThBe_{13}$ using pulsed magnetic fields and compare the results with new calculations of the electronic structure. The combination of a high electron density and a large unit cell leads to a complicated FS consisting of several sheets (see Fig. 4 for topographical views of these FS sheets). A comparison of the angle-dependent dHvA measurements with the calculations yields reasonable agreement, with parts of all four sheets being observable. As should be expected for a weakly interacting system, the majority of the effective masses are of order the free electron mass m_e, with the smallest pockets having subelectron effective masses. These values are still, nevertheless, double those predicted by band structure and are therefore suggestive of notable electron-phonon interactions. While the observation of LQO's in $ThBe_{13}$, down to magnetic fields as low as ~ 1 T, demonstrates that the detection system used in this study is of sufficient sensitivity for studying the dHvA effect in MBe_{13} compounds, the same technique, when applied to UBe_{13}, yields negative results. The consequences of these results are discussed, in the light of earlier claims of successful LQO measurements in UBe_{13}.

II. EXPERIMENT

The samples of $ThBe_{13}$ used for this study were grown from Th and Be dissolved in Al flux at 1200 °C. The same growth procedure is used for all MBe_{13} compounds. The Al flux was etched away using NaOH solution, and from the total yield of crystals (~ 5 cm^3) the smallest single crystals of dimensions $\sim 0.3 \times 0.3 \times 1$ mm^3 were chosen for the dHvA study for which the $\langle 100 \rangle$, $\langle 110 \rangle$, and $\langle 111 \rangle$ faces were clearly identifiable on inspection under a microscope. Pulsed magnetic fields were provided by the National High Magnetic Field Laboratory (NHMFL), Los Alamos, while angle-dependent dHvA measurements were made using a compensated set of dHvA coils that was able to be rotated with respect to the axis of the magnetic field B between pulses. Temperatures between 500 mK and 4 K were obtained by pumping on ^{3}He and ^{4}He reserviors.

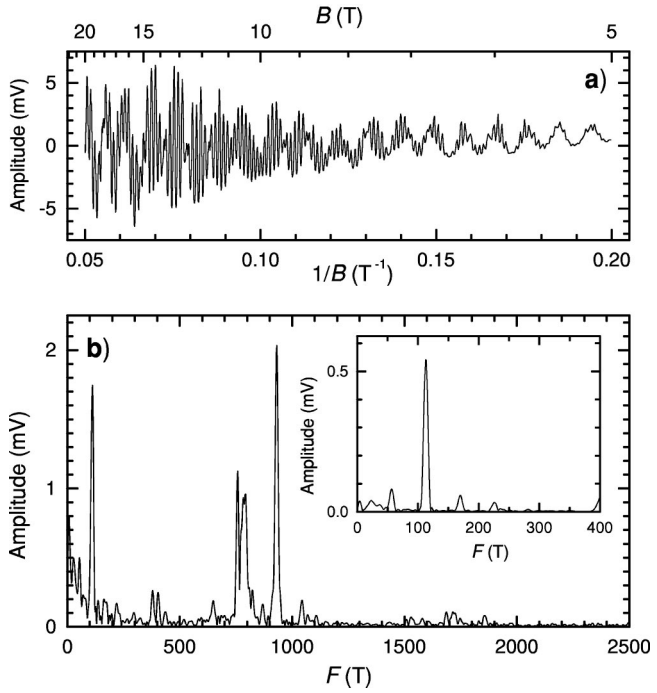

FIG. 1. (a) dHvA oscillations measured in $ThBe_{13}$ with B oriented to within 1° of the $\langle 100 \rangle$ crystallographic axis at 500 mK on the rising magnetic field. (b) A Fourier transformation of the dHvA signals in (a). The inset shows a Fourier transform of the oscillations measured at lower magnetic fields between 2 and 5 T.

An example of a dHvA signal observed on the rising side of a magnetic field pulse for B aligned within 1° of the $\langle 100 \rangle$ axis is shown in Fig. 1(a), with the Fourier transform shown in Fig. 1(b). Irrespective of interactions, each of the dHvA frequencies F is directly related to a particular semiclassical orbit in k space via the Onsager relation $F = A_k \hbar / 2\pi e$,[16] where A_k is the extremal FS cross-sectional area enclosed by the orbit. The presence of a plethora of frequencies in Fig. 1(b) is immediately indicative of a rather complicated FS topology. While the conventional cubic unit cell of $ThBe_{13}$, with lattice constant $\mathbf{a} \approx 10.383$ Å, contains 8 formula units, the crystal symmetry is equivalent to that of a FCC lattice for which the primitive unit cell contains only 2 formula units.[2] In the absence of magnetic breakdown effects[16], we should therefore expect all of the dHvA frequencies to be lower than the maximum cross-section area of the Brillouin zone [BZ (equivalent to ~ 14386 T at this orientation)]. This is evidently the case in Fig. 1(b).

III. ELECTRONIC STRUCTURE CALCULATIONS

The complicated spectrum of dHvA frequencies in Fig. 1(b) implies that a complete understanding of the FS topology together with the interactions would be untenable without the assistance of band structure calculations. Before discussing the angle-resolved dHvA data in detail, it is therefore necessary for us to present the results of recent calculations made on $ThBe_{13}$. The calculated band structure and density of states are shown in Figs. 2 and 3 respectively, while to-

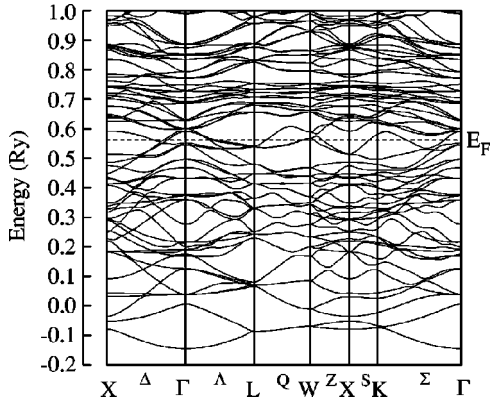

FIG. 2. The band structure of $ThBe_{13}$, calculated according to the method described in the text.

pographical views of the FS sheets are shown in Fig. 4.

In contrast to the earlier band structure calculations made on MBe_{13} (with M=La, Ce, Th and U),[2,31] the present calculations include the effects of spin-orbit interactions by means of a linear augmented-plane-wave (LAPW) method. The exchange-correlation potential was modeled by means of a local-density approximation (LDA), using the formula originally developed by Gunnarsson and Lundqvist.[32] Scalar relativistic effects were taken into account for all electrons, while the spin-orbit interactions were included for the valence electrons only as a secondary variational procedure. The muffin-tin (MT) radii for Th, Be-I and Be-II sites were set to $0.1846\times\mathbf{a}$, $0.1005\times\mathbf{a}$, and $0.1093\times\mathbf{a}$, respectively. Inside each of the MT spheres, the core electrons (Rn-core minus the $6p^6$ electrons in the case of Th and He-core in the case of Be) were calculated self consistently for each iteration. The $6p^6$ electrons in Rn were considered as valence electrons within the second energy window, where another set of LAPW basis functions is used. The LAPW basis functions were truncated at $|\mathbf{k}+\mathbf{G}_i|\leq 10.44\times 2\pi/\mathbf{a}$, where $\mathbf{G}_i$ is the reciprocal lattice vector, leading to a total of 1243 LAPW functions at the Γ point of the BZ. The sampling points were evenly distributed within the irreducible 1/48th of the first BZ, using 19 **k** points for the potential convergence and 231 **k** points for the final band structure.

Since the Th $5f$ components in $ThBe_{13}$ are located well above the Fermi level, as shown in Fig. 3, the Fermi surface,

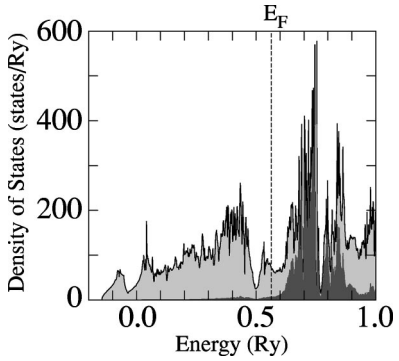

FIG. 3. The calculated density of states of $ThBe_{13}$. The lightly shaded (enclosed by a solid line) and heavily shaded regions indicate the total density of states and the partial contribution from Th f component (within the MT sphere), respectively.

which consists mainly of Be p bands, is little influenced by the effects of spin-orbit interactions. Moreover, the Be p bands do not appear to require a larger number of basis functions. The calculated band structure, in the vicinity of the Fermi level (see Fig. 2), is therefore very similar to that calculated with more limited basis functions not including the effects of spin-orbit interactions.[2]

IV. ANGLE-RESOLVED dHvA STUDIES

Similarities between the calculated and experimental dHvA frequencies become apparent in Figs. 5(a) and 5(b) where their angular dependences are compared. In Fig. 5(a), the sizes of the points scale with magnitude of the dHvA signals determined by taking the natural logarithm of the peaks in the Fourier transform spectra; all of the data were scanned systematically with no data points rejected. Some of the points, particularly at the lower frequencies, are subject to errors caused by higher levels of noise. Lines adjoin points for which a clear angle-dependence of particular features can be resolved, and the various orbits that are expected to originate from the four FS sheets are identified in Fig. 5(b) using a scheme of Greek letters.

The strongest dHvA signal observed has a frequency of $\sim 931\pm 5$ T when B is oriented close to the $\langle 100\rangle$ crystallographic axis. On inspection of Fig. 5(a), it becomes apparent that the closest predicted feature to this is the square electronlike orbit θ centered about the X point of the BZ, originating from the 30th sheet. The calculated frequency is only ~ 50 T (or $\sim 5\%$) larger than that obtained experimentally and has the correct field orientation dependence; i.e., the frequency increases on rotating B away from the $\langle 100\rangle$ axis. The additional pair of frequencies (of ~ 760 and ~ 780 T), just below θ, have less obvious origins. However, the lower of the two is observed to persist over a broad range of angles, reaching a maximum value of $\sim$ 800 T when B is aligned parallel with the $\langle 111\rangle$ axis. It is therefore likely that this particular feature originates from the distorted cubelike hole surface ε situated at the Γ point of the BZ (also from the 30th sheet). Only a single frequency is observed for this portion of the FS owing to its location at a point of high symmetry in the BZ. This leaves the higher of these two frequencies unassigned. As the sample is rotated by angles of $\sim 10°$ to $\sim 30°$ towards the $\langle 111\rangle$ axis, another frequency of ~ 800 T is observed to decrease slowly with angle. Such a behavior is expected for the η orbit (also originating from the from the 30th FS surface). A further much larger, almost angle-independent, frequency of ~ 1850 T in Fig. 5(a) can only originate from larger hole-like cross-sections (χ) of the 30th sheet close to the X point of the BZ.

Another strong dHvA signal is observed on rotating B by ~ 15 to $20°$ towards the $\langle 110\rangle$ axis which, according to Fig. 5(b), appears to originate from holes (β) in the 31st electron surface. The same holes can also account for the lowest of the cluster of frequencies (of ~ 300 to 400 T) that are observed when B is rotated by angles of between $\sim 10°$ and $\sim 30°$ towards the $\langle 111\rangle$ axis from $\langle 100\rangle$. One of the frequencies within this cluster may correspond to the δ orbit in Fig. 5(b). A further weak, but strongly angle-dependent, frequency is observed over the same angular interval having a value that varies between ~ 500 and 700 T, apparently re-

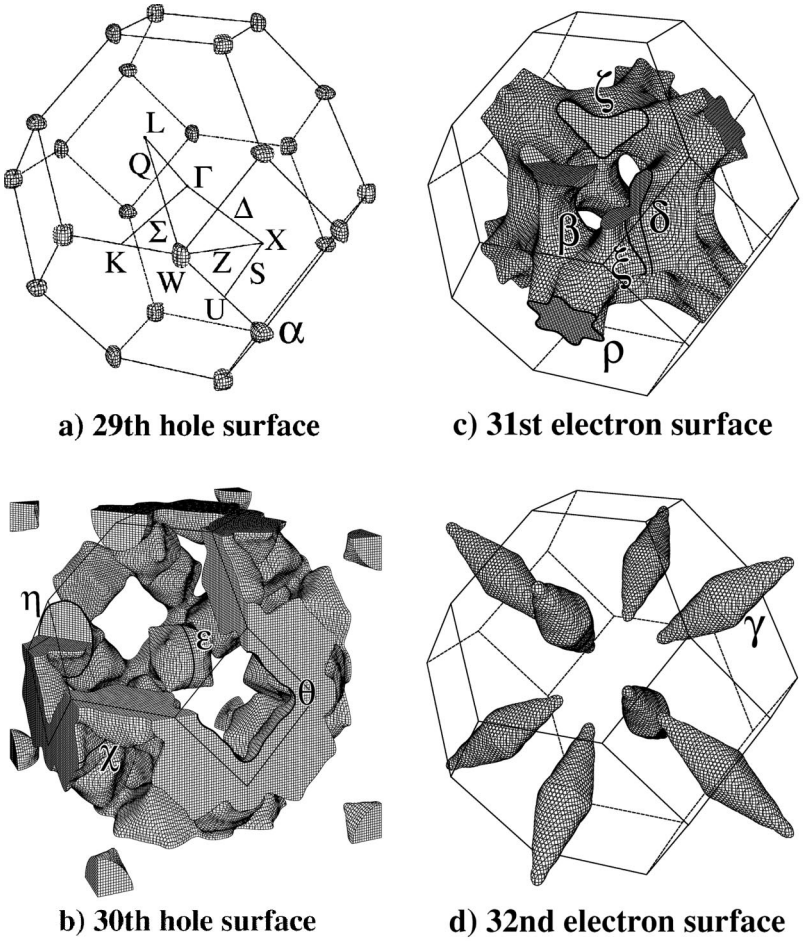

FIG. 4. Topographical views of the 29th to 32nd FS sheets constructed from the band-structure calculations.

sembling the behavior expected for the ρ orbit of the 31st sheet.

Perhaps the most striking agreement between the calculated and experimental FS's occurs in the case of the 32nd sheet, which consists of 8 electron ellipsoids (γ) situated at the L points of the BZ. When B is aligned close to $\langle 100 \rangle$, the frequencies (of $\sim$379 T) originating from all 8 ellipsoids are degenerate but, as depicted in Fig. 5(b), this frequency splits into two branches on rotating towards $\langle 110 \rangle$ or three on rotating towards $\langle 111 \rangle$. Such a pattern appears to be reproduced in Fig. 5(a), although some additional frequencies originate from the 31st electron surface, as discussed above. One of the γ frequencies dominates the dHvA spectrum when B is oriented close to the $\langle 110 \rangle$ axis.

We would normally expect smaller FS sections, such as the α hole pockets predicted for the 29th sheet, to be particularly susceptible to discrepancies between theory and experiment. In spite of this, low frequencies roughly of this order do appear to be present in Fig. 5(a), although there is some reduction in the signal-to-noise ratio over this region. The Fourier transform in the inset to Fig. 1(b) shows that the prominent frequency of $\sim$110 T in Fig. 5(a) is actually a second harmonic. Spin-splitting, which occurs when the Zeeman splitting energy becomes commensurate (or nearly commensurate) with an odd half-integer multiple of cyclotron energy $\hbar\omega_c$, is the most likely explanation for the attenuation of the fundamental frequency of $\sim$55 T. While this frequency and its harmonic are not present over the full angular range, it is within $\sim$20 T of that predicted from the calculated FS.

V. INTERACTIONS

As well as providing an accurate means for mapping out the FS topology of a metal, the dHvA effect provides valuable information on the nature of the low-lying quasiparticle interactions. In weakly correlated systems, a categorization that is expected to apply to $ThBe_{13}$, electron-electron interactions, and electron-phonon interactions usually manifest themselves as an enhancement of the effective masses with respect to those obtained from band structure calculations.[16] On increasing the temperature, the LQO's become damped owing to the increased width of the Fermi-Dirac distribution with respect to the Landau level separation energy $\hbar\omega_c$, where $\omega_c = eB/m^*$. In most three-dimensional metals, this leads to an additional thermal damping term $R_T = X_p/\sinh X_p$ in the expression for the dHvA effect amplitude, where $X_p = 2\pi^2 p k_B T/\hbar\omega_c$ (p being the harmonic index), to which experimental data can be fitted. The experimentally determined effective masses for B oriented close to $\langle 100 \rangle$ are compared with those obtained from the band-structure calculation in Table I. While the majority of the measured effective masses are close to the free electron mass m_e, they are still roughly twice those predicted by the band-structure calculations. Given the high-electron densities in $ThBe_{13}$ and the absence of a notable $5f$ electron contribu-

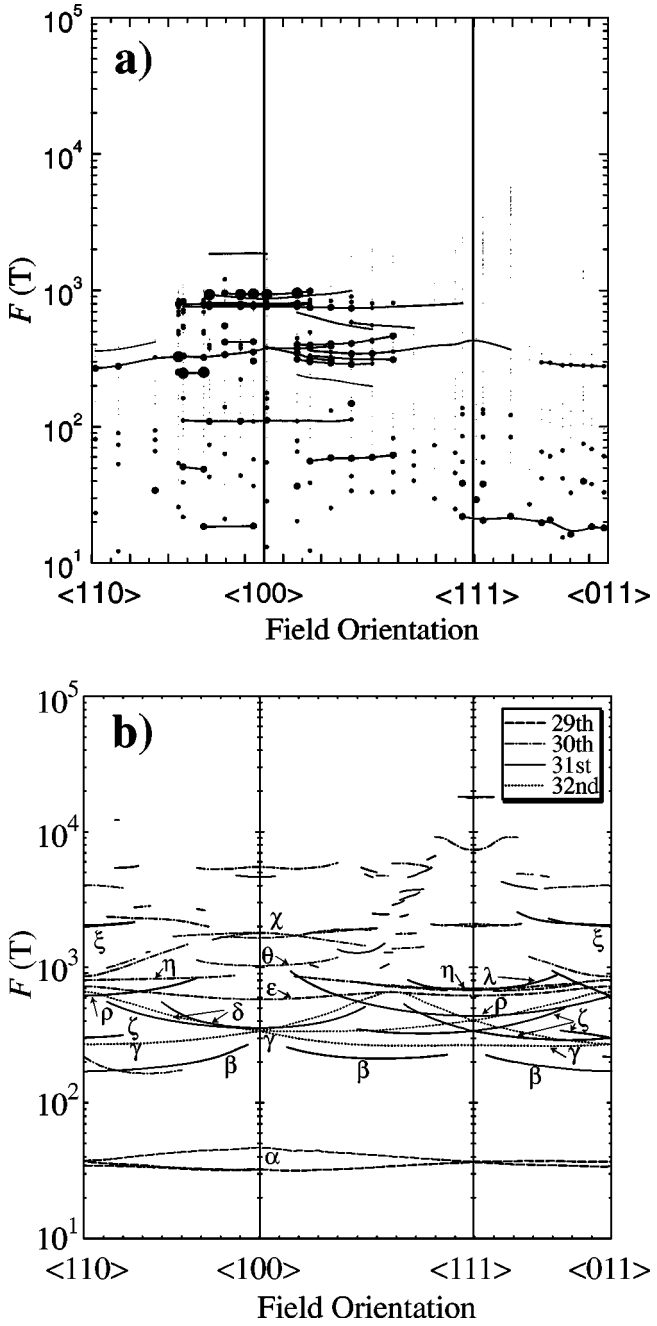

FIG. 5. (a) The measured peaks in the Fourier spectra at a range of different angles. The size of the circles represent the magnitude of the peaks, determined from the natural logarithm of the Fourier amplitudes. There is some degradation of the signal-to-noise ratio at lower frequencies. Lines have been drawn between some of the points in cases where very clear trends in the angle dependence of the frequencies are apparent. (b) Calculated angle dependence of the dHvA frequencies for the FS sheets shown in Fig. 4.

tion, it is more likely that the majority of the mass enhancement originates from electron-phonon interactions; although the molar specific heat of $ThBe_{13}$ is somewhat larger than that of most simple monatomic metals, this largely reflects the fact that one mole of MBe_{13} contains 14 atoms. Assuming the measured mass m^* to be related to the band mass m_b by the expression $m^* = m_b(1+\lambda^{EP})$,[16] we obtain from the average of all of the effective masses shown in Table I that $\lambda^{EP} \sim 1.0 \pm 0.3$. Given that λ^{EP} is of order unity, it is a surprising fact that $ThBe_{13}$ has not been reported to be a superconductor. LaB_{13} (which is electronically similar to $ThBe_{13}$[2]) has, nevertheless, been reported, following proximity effect experiments, to support the passage of Cooper pairs with exceptionally long lifetimes.[33] Within the MBe_{13} series, bulk superconductivity has only been reported in pure UBe_{13} and $U_{1-x}Th_xBe_{13}$ intermetallics, although it is questionable whether this is phonon mediated.

In addition to thermal effects, further damping of LQO's arises as a result of impurity scattering effects. Lorenzian broadening of the Landau levels, caused by finite relaxation times, leads to an exponential damping of the quantum oscillations; the damping term being $R_T = \exp(-2\pi^2 p k_B T_D/\hbar\omega_c)$. This is expressed in terms of a characteristic temperature $T_D = \hbar/2\pi k_B \tau$ by convention, but is easily convertible into an estimate of the quantum lifetime or the electron mean free path $l = v_F \tau$. These quantities, obtained by fitting to the field dependence of the experimental data (having corrected for the temperature dependence), are listed in Table I. The temperature dependence of a frequency is corrected for by dividing the experimentally measured amplitude by the thermal damping factor $R_T = X_p/\sinh X_p$, having inserted the appropriate effective mass for that orbit. Owing to the close proximity of some of the dHvA frequencies to one another in the Fourier transform, reliable Dingle temperatures can only be obtained for a few orbits. However, the mean free paths are approximately the same and of order ~ 1000 Å for all orbits. The short mean free paths in $ThBe_{13}$ probably reflect the difficulties encountered in producing pure defect-free single crystals of radioactive MBe_{13} compounds.

VI. IMPLICATIONS FOR UBe_{13}

One would expect that, having observed LQO's in $ThBe_{13}$, samples of UBe_{13} prepared under identical growth conditions should have similar mean free paths. The actinide starting materials have similar purities and both are chemically similar; i.e., have similar melting points and reactivities. Al impurities (originating from the flux), which tend to occupy some of the Be sites (as determined by x-ray diffraction experiments), are thought to be the primary type of impurity in these compounds. Thus, one would expect, on the basis of these considerations, to stand a reasonable chance of observing LQO's in UBe_{13} provided that the experimental conditions are right.

To the contrary, experiments performed on UBe_{13} in magnetic fields as high as 60 T and temperatures below ~ 500 mK using the same experimental apparatus yield no evidence for any LQO's. Should UBe_{13} retain its high effective mass and non-Fermi liquid-like properties in strong magnetic fields, the absence of LQO phenomena would be of no surprise. Were, on the other hand, the earlier reports of LQO effects in UBe_{13} actually genuine,[12,13] i.e., with effective masses even lower than those in $ThBe_{13}$, then LQO's should be easily observable in UBe_{13}, especially in view of the fact that the signal-to-noise ratio of the dHvA oscillations in $ThBe_{13}$ is at least of order 10 to 100.

The lack of dHvA data in the present UBe_{13} crystals therefore confirms the fact that the previously published LQO's were actually due to Al inclusions[14] and that the

TABLE I. A list of experimental and calculated frequencies F and effective masses m^* for B oriented close to $\langle 100 \rangle$. Dingle temperatures T_D, scattering rates τ^{-1}, Fermi velocities v_F, and mean free paths l are also shown.

Orbit	Sheet	F_{meas} (T)	F_{calc} (T)	m^*_{meas} (m_e)	m^*_{calc} (m_e)	T_D (K)	τ^{-1} (10^{12} s^{-1})	v_F (10^6 ms^{-1})	l Å
α	29th	55 ± 5	32 or 47	0.07 ± 0.01	0.10	7.0 ± 0.5	5.7	0.67	1182
ϵ	30th	759 ± 3	578	0.60 ± 0.05	0.23	3.5 ± 0.5	3.3	0.29	880
θ	30th	931 ± 3	1027	0.57 ± 0.03	0.27	6.5 ± 0.5	5.3	0.34	642
χ	30th	1853 ± 5	1800	1.16 ± 0.10	0.80			0.24	
δ	31st	402 ± 6	357	0.72 ± 0.05	0.35			0.18	
γ	32nd	379 ± 7	339	0.72 ± 0.05	0.35			0.22	

present samples are free from such inclusions. The samples used in this particular study were of much smaller cross-section ($\sim 10^{-7}$ m^2), in order to avoid eddy current heating problems and field-inhomogeneities, and so were unlikely to contain such inclusions. The absence of dHvA oscillations in UBe_{13} is more likely to reflect the fact that the effective masses are still exceptionally large at high magnetic fields (~ 300 m_e according to specific heat measurements) or that the ground state cannot exhibit LQO's because it is not a Fermi liquid.

VII. CONCLUSION

The dHvA studies on $ThBe_{13}$ in this paper have shown that this material is a normal metal albeit with a complicated FS and what appear to be notable electron-phonon interactions. The mean free paths of order 1000 Å, being very typical for binary alloys, make the prospects for observing LQO's in other MBe_{13} materials rather promising. The observation of such phenomena in UBe_{13} may either require much lower temperatures, because of the heavy effective masses, or may require measurements to be made in the extreme high magnetic field regime where the magnetization becomes saturated and spin fluctuation effects are suppressed.

ACKNOWLEDGMENTS

Work conducted at the National High Magnetic Field Laboratory was supported by the National Science Foundation (NSF), the State of Florida, and the Department of Energy (DOE). Other work at Los Alamos was performed under the auspices of the DOE. One of us (J.A.D) would like to thank Alex Lacerda through the CMS/DOE summer internship program for support.

[1] E. Bucher, J. P. Maita, G. W. Hull, R. C. Fulton, and A. S. Cooper, Phys. Rev. B **11**, 440 (1975).
[2] K. Takegahara, H. Harima, and T. Kasuya, J. Phys. F **16**, 1691 (1986).
[3] H. R. Ott, H. Rudigier, Z. Fisk, and J. L. Smith, Phys. Rev. Lett. **50**, 1595 (1983).
[4] G. R. Stewart, Rev. Mod. Phys. **56**, 755 (1984).
[5] Z. Fisk, H. R. Ott, T. M. Rice, and J. L. Smith, Nature (London) **320**, 124 (1986).
[6] D. L. Cox and M. Jarrell, J. Phys.: Condens. Matter **8**, 9825 (1996).
[7] F. Bommeli, L. Degiorgi, P. Wachter, F. B. Anders, and A. V. Mitin, Phys. Rev. B **56**, R10 001 (1997).
[8] A. Schiller, F. B. Anders, and D. L. Cox, Phys. Rev. Lett. **81**, 3235 (1998).
[9] G. R. Stewart, Z. Fisk, J. L. Smith, J. O. Willis, and M. S. Wire, Phys. Rev. B **30**, 1249 (1984).
[10] A. Hiess, M. Bonnet, P. Burlet, E. Ressouche, J.-P. Sanchez, J. C. Waerenborgh, S. Zwirner, F. Wastin, J. Rebizant, G. H. Lander, and J. L. Smith, Phys. Rev. Lett. **77**, 3917 (1996).
[11] G. Krill, J. P. Kappler, M. F. Ravet, A. Amamou, and F. Meyer, J. Phys. F **10**, 1031 (1980).
[12] B. Wolf, R. Blick, G. Bruls, B. Lüthi, Z. Fisk, J. L. Smith, and H. R. Ott, Z. Phys. B **85**, 159 (1991).
[13] G. M. Schmiedeshoff, Z. Fisk, and J. L. Smith, Phys. Rev. B **49**, 658 (1994).
[14] See G. G. Lonzarich, J. Magn. Magn. Mater. **76&77**, 1 (1988); M. Springford, Physica B **171**, 151 (1991).
[15] R. Corcoran, P. Meeson, P. A. Probst, M. Springford, B. Wolf, R. Blick, G. Bruls, B. Lüthi, Z. Fisk, J. L. Smith, and H. R. Ott, Z. Phys. B **91**, 135 (1993).
[16] D. Shoenberg, *Magnetic Oscillations in Metals* (Cambridge University Press, Cambridge, 1984).
[17] A. Wasserman and M. Springford, Adv. Phys. **45**, 471 (1996).
[18] H. Aoki, S. Uji, A. K. Albessard, and Y. Onuki, Phys. Rev. Lett. **71**, 2110 (1993).
[19] T. Terashima, C. Howarth, M. Takashita, H. Aoki, N. Sato, and T. Komatsubara, Phys. Rev. B **55**, R13 369 (1997).
[20] R. G. Goodrich, N. Harrison, A. Teklu, D. Young, and Z. Fisk, Phys. Rev. Lett. **82**, 3669 (1999); N. Harrison, D. W. Hall, R. G. Goodrich, J. J. Vuillemin, and Z. Fisk, *ibid.* **81**, 970 (1998).
[21] D. M. Edwards and A. C. M. Green, Z. Phys. B **103**, 243 (1997).
[22] J. Spałek, P. Korbel, and W. Wójcik, Phys. Rev. B **56**, 971 (1997).
[23] G. M. Schmiedeshoff, Z. Fisk, and J. L. Smith, Phys. Rev. B **48**, 16 417 (1993).
[24] J. A. Detwiler, G. M. Schmiedeshoff, N. Harrison, A. H. Lacerda, J. C. Cooley and J. L. Smith (unpublished).
[25] J. L. Smith, Z. Fisk, J. O. Willis, B. Batlogg, and H. R. Ott, J. Appl. Phys. **55**, 1996 (1984).
[26] R. H. Heffner, J. L. Smith, J. O. Willis, P. Birrer, C. Baines, F. N.

Gygax, B. Hitti, E. Lippelt, H. R. Ott, A. Schenck, E. A. Knetsch, J. A. Mydosh, and D. E. MacLaughlin, Phys. Rev. Lett. **65**, 2816 (1990).

[27] H. R. Ott, H. Ruigier, Z. Fisk, and J. L. Smith, Phys. Rev. B **31**, 1651 (1985).

[28] I. A. Luk'yanchuk and V. P. Mineev, Pis'ma Zh. Éksp. Teor. Fiz. **47**, 460 (1988) [JETP Lett. **47**, 543 (1988)].

[29] F. Kromer, R. Helfrich, M. Lang, F. Steglich, C. Langhammer, A. Bach, T. Michels, J. S. Kim, and G. R. Stewart, Phys. Rev. Lett. **81**, 4476 (1998).

[30] E.-W. Scheidt, T. Schreiner, P. Kumar, and G. R. Stewart, Phys. Rev. B **58**, 15 153 (1998).

[31] K. Takegahara, H. Harima, and T. Kasuya, J. Magn. Magn. Mater. **47&48**, 263 (1985).

[32] O. Gunnarsson and B. I. Lundqvist, Phys. Rev. B **13**, 4276 (1976).

[33] S. Han, K. W. Ng, E. L. Wolf, H. F. Braun, L. Tanner, Z. Fisk, J. L. Smith, and M. R. Beasley, Phys. Rev. B **32**, 7567 (1985).